Available online at www.sciencedirect.com

ScienceDirect

International Journal of Thermal Sciences 48 (2009) 514–520

International Journal of Thermal Sciences

www.elsevier.com/locate/ijts

Streaming flows in differentially heated square porous cavity under sinusoidal g-jitter

Pradyumna Ghosh *, M.K. Ghosh

Department of Mechanical Engineering, Institute of Technology, BHU, Varanasi 221005, India

Received 23 November 2007; received in revised form 16 April 2008; accepted 16 April 2008

Available online 3 June 2008

Abstract

Transient transport phenomenon in a square porous cavity under sinusoidal g-jitter has been solved numerically. Sinusoidal g-jitter introduces a true periodic behavior to the average Nusselt number. Pulsating wave from hot and cold side travels to-wards the center and almost in the center of the cavity the two waves engage in constructive/destructive interference leading to the formation of stationary wave. Sinusoidal g-jitter creates the streaming flows inside the porous cavity and time-dependent rolls have been observed inside the cavity due to differences in thermal diffusivities among solid matrix, wall and the fluid.

Keywords: Square porous cavity; Sinusoidal g-jitter; Pulsating wave; Streaming flows; Time-dependent rolls

1. Introduction

Microgravity indicates low gravity, where the mean gravitational acceleration is in the range of 10^{-1}–10^{-5} m/s^2. All onboard objects experience low amplitude broadband perturbed acceleration, or g-jitter, where there is a non-zero steady part and a oscillatory part. Internal natural convection is a phenomenon of natural convection in an enclosure which has immense potential of engineering applications. Generally, it is classified into two broad category viz. enclosures heated from the side wall and enclosures heated from below. In enclosures heated from the side, buoyancy driven flow is initiated even due to a very small temperature imposed between the two side walls whereas in enclosures heated from below a critical temperature must be imposed prior to detection of flow and convective heat transfer. The hierarchy of flow regimes and various transition in convection usually known as Bénard convection has been reviewed by Busse [5]. In porous cavity heated from the side all four convection regimes viz. pure convection, tall layers, high Raleigh convection and shallow layers were investigated by Bejan and Tien [3] for which results were presented in the parametric form. Natural convection in porous medium heated from below was investigated by Cheng [6]. Kamotani, Prasad and Ostrach [12] have analyzed two-dimensional square cavity convection with zero mean gravity acceleration using small amplitude linearized equations for the fluctuating field and steady state equations for the mean field. The mathematical model is considered to give good prediction of the system behavior at low values of the vibrational Rayleigh number. Their results correspond to the fact that there is no threshold for the onset of convection inside the cavity with horizontally applied temperature gradient (g-jitter is perpendicular to the thermal gradient) but there is a threshold for vertically applied thermal gradient, i.e. parallel to g-jitter. Gershuni and Zhukhovitskiy [8] presented a summary of the studies done by several Russian researchers covering analytical and fully nonlinear numerical investigations. These analytical works were based on the method of averaging under the assumption of high frequency g-jitter. Biringen and Danabasoglu [4] solved fully nonlinear time-dependent Boussinesq equations for g-jitter in a two-dimensional rectangular cavity with an aspect ratio of 2 at $Ra = 1.775 \times 10^5$ and at a Prandtl number $(Pr) = 0.007$ (liquid germanium). They specified the critical value of ω above which the system experiences transition from convective temperature

* Corresponding author.
E-mail addresses: pradyumna_ghosh@rediffmail.com (P. Ghosh), mkghosh47@yahoo.com (M.K. Ghosh).

1290-0729/$ – see front matter
doi:10.1016/j.ijthermalsci.2008.04.002

Nomenclature

C_{pf}	specific heat of fluid	kJ/kg K
C_s	specific heat of solid matrix	kJ/kg K
K	permeability of the porous media	m^2
k	thermal conductivity	W/m K
k_f	thermal conductivity of the fluid filled in the pore	W/m K
k_s	thermal conductivity of the solid matrix	W/m K
k_{eff}	thermal conductivity of porous matrix saturated with fluid	W/m K
Nu_{av}	average Nusselt number	
Ramod	Darcy–Rayleigh number	
g	effective gravitational acceleration, mean value of g-jitter,	m/s^2
g_0	gravitation acceleration at earth	m/s^2
Pr	Prandtl number, ν_f/α_e	
T	temperature/temperature of the fluid saturated porous media	°C
T_c	cold wall temperature	°C
T_h	hot wall temperature	°C
T_o	reference temperature	°C
t^*	dimensionless time, $t^* = t\ (\alpha_e/W^2\sigma)$	
u^*	x-component dimensionless velocity	
v^*	y-component dimensionless velocity	
v_0	reference velocity, α_e/W	
W	width and height of the cavity	m
x	horizontal distance	m
x^*	dimensionless horizontal distance	
y^*	dimensionless vertical distance	
y	vertical distance	m
P	pressure	Pa
P^*	dimensionless pressure	

Greek symbols

α_e	thermal diffusivity of the homogeneous, isotropic, porous medium	m^2/s
β	thermal expansion coefficient of the fluid	$°C^{-1}$
θ^*, θ	dimensionless temperature	
ν	kinematic viscosity of the fluid	m^2/s
μ	viscosity	$N\,s/m^2$
ω	angular frequency	Hz
ω^*	dimensionless angular frequency, $\omega^* = \omega\sigma W^2/\alpha_e$	
ρ	density of the fluid	kg/m^3
ρ_o	density of the outer fluid of the convection region	kg/m^3
ρ_s	density of solid matrix	kg/m^3
σ	dimensionless combined homogeneous porous media specific heat/unit volume	

fields to a conductive one. Kondos and Subramanian [13] have investigated the effect of frequency with g-jitter perpendicular to the applied thermal gradient in two-dimensional square cavity. They showed that there are qualitative differences in flow field between low and high frequencies. A detailed flow field and heat transfer analysis under g-jitter with a zero-mean base gravity parallel to the applied thermal gradient inside the enclosure has been studied by Hirata et al. [11] which also includes the analysis of onset of convection. The nonlinear analysis of onset of convection of the system revealed rich dynamics even at a low Ra and ω. Ruiz et al. [17] described natural convection in fluid filled cavity as the limiting case of vibro-convective flow patterns where gravity acts normal to the thermal gradient.

Combarnous and Bories [7] investigated on hydrothermal convection in porous media. Convection in porous cavity was also investigated by Walker and Homsy [18]. Gross, Bear and Hickox [10] dealt with the application of flux corrected transport (FCT) to high Rayleigh number natural convection in porous medium. Moya, Ramos and Sen [16] conducted a numerical study of natural convection in a tilted porous material.

Manole and Lage [14] presented numerical bench mark results for natural convection in a porous medium cavity. Baytas and Pop [2] studied free convection in oblique enclosures filled with a porous medium. Mahmud and Fraser [15] have discussed the effect of entropy generation in a square porous cavity under transverse gravitational acceleration.

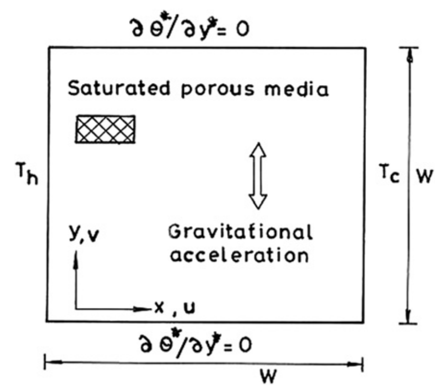

Fig. 1. Schematic diagram of the square porous cavity under sinusoidal g-jitter.

However, there is no reported research activity on buoyancy driven flow under the influence of g-jitter perpendicular to the applied thermal gradient in square porous cavity as of today. In the present investigation, unique convection pattern, inside a porous cavity under the influence of g-jitter perpendicular to the applied thermal gradient where the base microgravity ($10^{-6}g_0$) has been determined by solving transport equations numerically [9].

2. Transport equations and solution methodology

Fig. 1 shows the domain to be analyzed and the adopted coordinate system. Fluid in a two-dimensional cavity with square cross section is subjected to g-jitter parallel to Y-axis. Upper and lower walls parallel to the X-axis are adiabatic. Left and right walls are isothermal but have different temperatures and it has been also assumed that isothermal walls are perfect conductor of heat. It is assumed that the cavity is completely filled with homogeneous porous media saturated with Newtonian fluid. The aspect ratio (height/width) of the cavity is 1. Uneven density of fluid originating from the temperature difference of the walls produces buoyancy and drives the convection. The saturated porous medium is assumed to be isotropic in thermal conductivity and follows the Darcy model (A. Bejan [1]).

According to Darcy's law it has been observed that, x directional pore velocity is proportional to the imposed pressure gradient and y directional pore velocity is proportional to imposed pressure gradient and static pressure gradient. However, the x directional pore velocity (u) and y directional pore velocity (v) can be presented as follows,

$$u = \frac{K}{\mu}\left(-\frac{\partial p}{\partial x}\right) \tag{1}$$

$$V = \frac{K}{\mu}\left(-\frac{\partial p}{\partial y} + \rho g\right) \tag{2}$$

Using Darcy's law the dimensionless transport equations under sinusoidal g-jitter are as follows.

All asterisked quantities and θ in this paper are in dimensionless form

$$\frac{\partial u^*}{\partial x^*} + \frac{\partial V^*}{\partial y^*} = 0 \tag{3}$$

$$u^* = -\frac{\partial p^*}{\partial x^*} \tag{4}$$

$$V^* = -\frac{\partial p^*}{\partial y^*} + Ra \bmod \theta \sin(\omega^* t^*) \tag{5}$$

$$\frac{\partial \theta^*}{\partial t^*} + u^*\left(\frac{\partial \theta^*}{\partial x^*}\right) + V^*\left(\frac{\partial \theta^*}{\partial y^*}\right) = \frac{\partial^2 \theta^*}{\partial x^{*2}} + \frac{\partial^2 \theta^*}{\partial y^{*2}} \tag{6}$$

where, $u^* = u/v_0$, $V^* = v/v_0$, $t^* = t\ (\alpha_e/W^2\sigma)$, $x^* = x/W$, $y^* = y/W$.

$$\Delta T = T_h - T_c, \qquad T_0 = T_c, \qquad \theta^* = (T - T_0)/\Delta T$$

$$\omega^* = \omega\sigma W^2/\alpha_e, \qquad p^* = \frac{p}{\rho(\nu/W)^2}$$

$$\theta = (T_h + T_c)/2\Delta T, \qquad \alpha_e = \frac{k_{\text{eff}}}{\rho_f c_{pf}}$$

$$k_{\text{eff}} = \left[\varepsilon k_f + (1-\varepsilon)k_s\right], \qquad v_0 = \alpha_e/W$$

$$\text{Ramod} = \frac{gK\beta\Delta T W}{\alpha_e \upsilon}, \qquad \sigma = \frac{[\varepsilon\rho_f c_{pf} + (1-\varepsilon)\rho_s c_s]}{\rho_f c_{pf}} \tag{7}$$

Subjected, to following initial and boundary conditions:

Initial conditions:

$t = 0$

$0 \leqslant x^* \leqslant 1, \quad 0 \leqslant y^* \leqslant 1, \quad u^* = 0, \quad v^* = 0$

$y^* = 0, \quad 0 \leqslant x^* \leqslant 1, \quad \partial\theta^*/\partial y^* = 0$

$y^* = 1, \quad 0 \leqslant x^* \leqslant 1, \quad \partial\theta^*/\partial y^* = 0$

$x^* = 0, \quad 0 \leqslant y^* \leqslant 1, \quad \theta^* = 0$

$x^* = 1, \quad 0 \leqslant y^* \leqslant 1, \quad \theta^* = 0$

Boundary conditions:

$t > 0$

$y^* = 0, \quad 0 \leqslant x^* \leqslant 1, \quad \partial\theta^*/\partial y^* = 0$

$v^* = 0, \quad u^* = 0$ (no slip boundary condition)

$y^* = 1, \quad 0 \leqslant x^* \leqslant 1, \quad \partial\theta^*/\partial y^* = 0$

$v^* = 0, \quad u^* = 0$ (no slip boundary condition)

$x^* = 0, \quad 0 \leqslant y^* \leqslant 1, \quad \theta^* = 1$

$u^* = 0, \quad v^* = 0$ (no slip boundary condition)

$x^* = 1, \quad 0 \leqslant y^* \leqslant 1, \quad \theta^* = 0$

$u^* = 0, \quad v^* = 0$ (no slip boundary condition)

$$Nu(y^*) = \partial\theta^*/\partial x^*; \qquad Nu_{\text{av}} = \int_0^1 (\partial\theta^*/\partial x^*)\, dy^*$$

A modular computer code has been designed to solve 2-D transient single-phase incompressible flow and heat transfer for a finite volume not too deviating from orthogonal shape. In this code, initially x directional velocity (u) and y directional velocity (v) have been calculated directly for a guessed pressure field and accurate velocity and the pressure field will be calculated after satisfying the continuity equation through a iterative procedure. Newton–Rapson and line solver has been used for the energy equation which uses the combination of central difference and upwind difference with weighting factors. The transient terms have been discritized using Crank–Nikolson method which is unconditionally stable and requires no restriction on time step, however relatively small time step has been considered to capture the local transport phenomenon. The resulting algebraic equations are solved by Thomas algorithm/TDMA integrating over number of time steps for the given increment of time. The pressure equation is derived from substituting the momentum equations into the continuity equation and the pressure-correction has been introduced using the principle that, the stream wise velocity is proportional to dp/dx. Hence, a correction of $u(i, j)$, which is determined by mass balance, should also correspond to a correction of dp/dx. Converged condition has been achieved when the difference in the two successive iterative value of a particular scalar variable is less than 10^{-6}. Mesh independent solution has been achieved using different mesh sizes for the prescribed computational domain.

3. Numerical results

Results are presented for three Ramod = 10, 100, 1000. The whole computational domain is subdivided into rectangular mesh with a size of 120×120. The convergence of the numerical solution with respect to mesh fineness is shown in Table 1. However, regarding the time step it has been unconditionally stable as Crank–Nikolson method has been used. Average Nusselt numbers (Nu_{av}) have been calculated in discrete time steps rather than in a continuous time scale to reduce the computation time.

Table 1
Convergence of the numerical solution with respect to mesh fineness for Ramod $= 10, 100$ ($\sin(\omega t) = 1$)

Darcy–Rayleigh number (Ramod)	Mesh points	Nu_{av}
10	80×80	1.07
	100×100	1.07
	120×120	1.07
100	80×80	3.07
	100×100	3.12
	120×120	3.14

Table 2
Comparison of average Nusselt number with some previous numerical results at constant gravity ($\sin(\omega t) = 1$)

	Ramod = 10	Ramod = 100	Ramod = 1000
Baytas and Pop [2]	1.07	3.16	14.06
Walker and Homsy [18]	–	3.10	12.96
Gross et al. [10]	–	3.14	13.45
Manole and Lage [14]	–	3.12	13.64
Moya et al. [16]	1.07	2.80	
Mahmud and Fraser [15]	1.07	3.14	13.82
Present prediction [9]	1.07	3.14	13.80

For bench-marking purpose, a differentially heated square porous cavity under constant gravitational acceleration is considered, average Nusselt numbers (Nu_{av}) have been calculated for three different Darcy–Rayleigh's numbers (Ramod $=$ 10, 100 and 1000) and compared with the available published works [2,10,14–16,18]. This comparison is shown in Table 2. It has been observed from the table that the agreement between present and previous result is very good. However, plotted streamline contour inside the porous cavity at constant gravity ($\sin(\omega t) = 1$) has been compared with the previously published result [16] successfully.

It has been also observed from practical considerations of porous media that Darcy–Rayleigh number (Ramod) ranges between (10–10^3). Rate of heat transfer is measured in terms of the average Nusselt number. In case of square porous cavity heated from the side, convection starts whenever there is an imposed temperature difference. So, study of onset of convection is not that important in this particular configuration, however, once gravity oscillation is introduced it takes some time to set the convection motion inside the cavity. For a limited time interval $0 < t^* \leqslant 3$, variation of average Nusselt number (Nu_{av}) is reported as a function of dimensionless time (t^*) in Fig. 2 for two different Ramod $= 100$ and 1000. It is evident from Fig. 2 that, an induced gravity oscillation introduces a true periodic behavior to the average heat transfer rate inside the cavity. Fig. 3 also indicates that, the periodic response of average Nusselt number (Nu_{av}) is synchronized with the forced acceleration, namely, having the same period as the forced acceleration. At the upper extreme of oscillation ($\omega t^* = (2m-1)\pi/2$, $m = 1, 2, 3, \ldots$) the magnitude of Nu_{av} approaches the corresponding value of Nu_{av} at steady state and constant gravity. Effect of ω on Nu_{av} is shown in Fig. 3 for Ramod $= 100$. Two extreme Nusselt numbers remain same for both values of ω. These figures indicate that, at the lower extreme of the oscillation, gravity force almost disappears ($\omega t^* = m\pi$, $m = 1, 2, 3, \ldots$). Heat transfer inside the cavity occurs in conduction mode. For all Ramod, Nu_{av} is same almost equal to 1 (which is the Nusselt number during any conduction heat transfer) whereas the convection/diffusion occurs at the upper extreme of the oscillations.

4. Streaming flow inside the square porous cavity under sinusoidal g-jitter

Transient transport phenomenon feature for a square porous cavity under constant micro-gravity ($10^{-6} g_0$) has been compared with transport phenomenon feature for a porous cavity

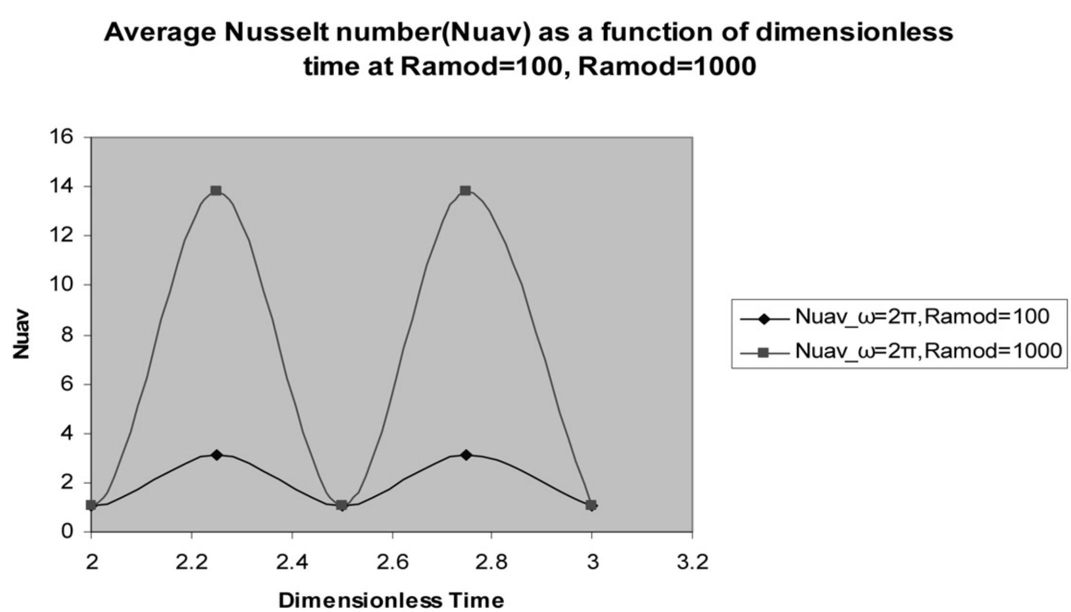

Fig. 2. Average Nusselt number (Nu_{av}) as a function of dimensionless time at $\omega = 2\pi$ and Ramod $= 100$ and 1000.

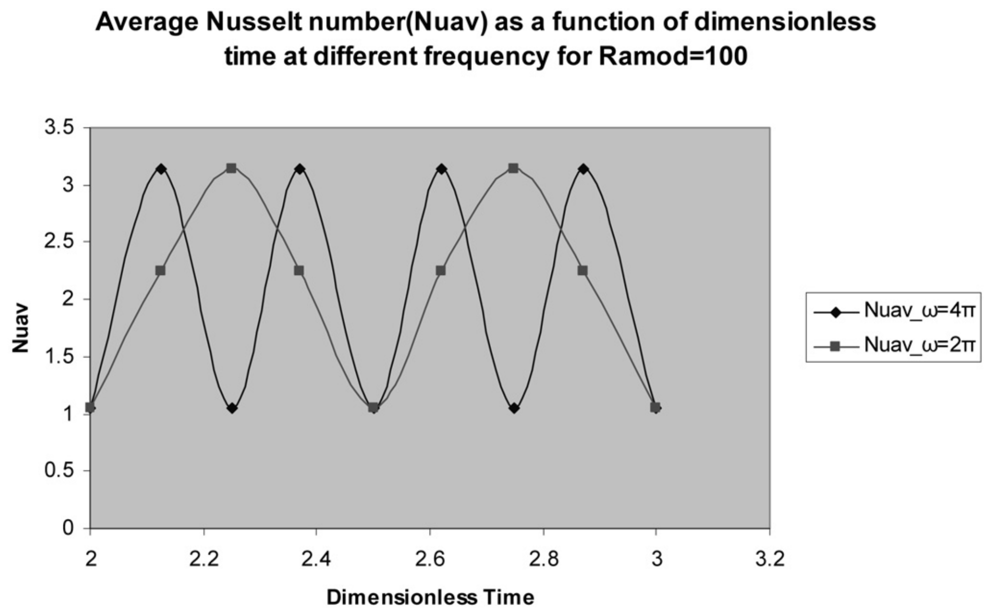

Fig. 3. Average Nusselt number (Nu_{av}) as a function of dimensionless time at $\omega = 2\pi$ and 4π and Ramod $= 100$.

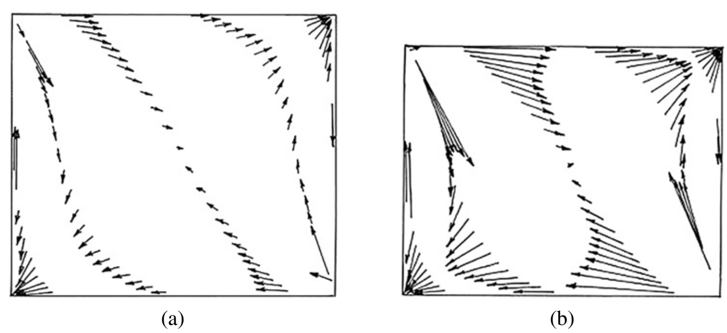

Fig. 4. (a) Velocity vectors in porous cavity at constant $g = 10 \times 10^{-6}$ m/s^2 at 0.1 s. (b) Velocity vectors in porous cavity at constant $g = 10 \times 10^{-6}$ m/s^2 at 0.5 s.

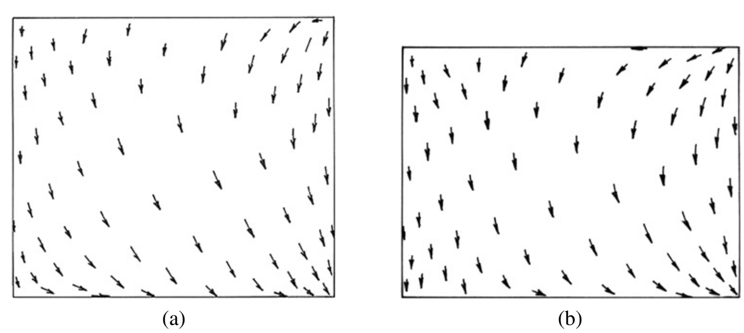

Fig. 5. (a) Velocity vectors in porous cavity at Ramod $= 100$, $\omega = \pi/2$, 0.05 s. (b) Velocity vectors in porous cavity at Ramod $= 100$, $\omega = \pi/2$, 0.7 s.

under sinusoidal g-jitter to identify the unique streaming flow feature.

4.1. Transient transport phenomenon feature for a porous cavity under constant micro-gravity ($10^{-6} g_0$)

Transient transport phenomenon in porous cavity under constant micro-gravity has been shown in Fig. 4 (a), (b). Transient rolls have been observed along the two vertical walls due to the difference of thermal diffusivities of solid and fluid. In the mid-plane of the cavity at the upper half, flow is from hot side to cold wall and in the lower half the flow is from cold side to hot wall, which clearly indicate a clockwise rotation. However, it has been observed that after 0.5 s (flow time) there is no significant quantitative change in the velocity vectors.

4.2. Transient transport phenomenon feature for a porous cavity under sinusoidal g-jitter

In the present investigation, *streaming flow* has been observed due to thermal convection at the start and end of a period of oscillation which has been described in Fig. 5 (a), (b). Pul-

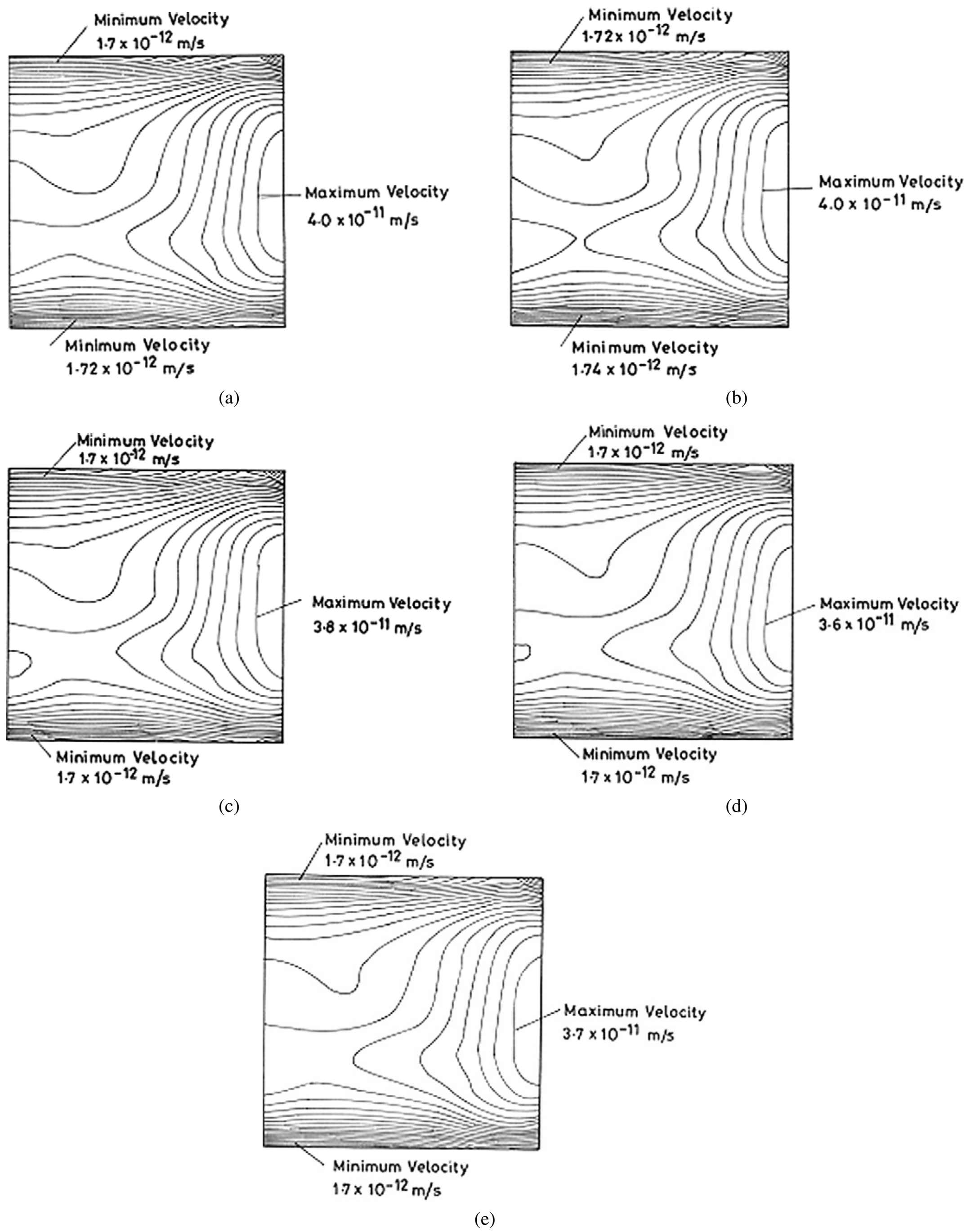

Fig. 6. (a) Velocity contour at 0.05 s, Ramod = 100, $\omega = \pi/2$. (b) Velocity contour at 0.15 s, Ramod = 100, $\omega = \pi/2$. (c) Velocity contour at 0.4 s, Ramod = 100, $\omega = \pi/2$. (d) Velocity contour at 0.6 s, Ramod = 100, $\omega = \pi/2$. (e) Velocity contour at 0.7 s, Ramod = 100, $\omega = \pi/2$.

sating wave from hot and cold side travels to the center and almost at the center of the cavity the two waves engage in constructive/destructive interference leading to the formation of a stationary wave [Fig. 6 (a)–(e)]. The period of oscillation for this entire phenomenon is 0.65 s, which is quite obvious from Fig. 6. The excitation frequency of the forcing function is about 0.25 Hz where as the response frequency is 1.54 Hz (for a time period of 0.65 s), which is quite obvious in case of nonlinear system response. However, FFT analysis has been carried out for individual monitoring stations which clearly indicate that, sub-harmonics are present in system response. However, it is not necessary for its to match with the thermal pulsating wave propagation frequency in the porous cavity. Uniqueness of the transport phenomenon in case of the porous cavity is the streaming and transient rolls due to difference in thermal diffusivities of solid matrix, wall and the fluid.

5. Conclusions

A numerical solution of the governing mass, transient momentum and energy equation for a porous square cavity under gravity oscillation has been presented to show the transient fluid flow and heat transfer response. Gravity oscillation introduces a true periodic behavior to the Nusselt number. The periodic response of Nusselt number is synchronized with the forced acceleration, having the same period as of forced acceleration. At the upper extreme of the oscillation, the magnitude of Nu_{av} approaches the corresponding value of Nu_{av} at steady state and constant gravity, and at the lower extreme of the oscillation gravity force disappears then heat transfer inside the cavity occurs in conduction mode. Under g-jitter effect on differentially heated square porous cavity, pulsating wave from hot and cold side travels to the center and almost at the center of the cavity the two waves engage in constructive/destructive interference leading to the formation of a stationary wave. Moreover, streaming flow has been observed inside the cavity. Transient rolls have been observed inside the porous cavity due to difference in thermal diffusivities of solid matrix, wall and the fluid. However, analysis of the transient response of velocity for $\omega = \pi/2$ at different monitoring stations indicates that near the upper adiabatic wall and near the center sub-harmonic frequencies are involved with the base frequency of g-jitter similar to nonlinear system.

References

[1] A. Bejan, Convection Heat Transfer, John Wiley & Sons, New York, 1984.

[2] A.C. Baytas, I. Pop, Free convection in oblique enclosures filled with a porous medium, Int. J. Heat Mass Transfer 42 (1999) 1047–1057.

[3] A. Bejan, C.L. Tien, Natural convection in horizontal porous medium subjected to an end to end temperature difference, J. Heat Transfer 100 (1978) 191–198.

[4] S. Biringen, G. Danabasoglu, Computation of convective flow with gravity modulation in rectangular cavities, J. Thermophys. 4 (1990) 357–365.

[5] F.H. Busse, Non-linear properties of thermal convection, Rep. Prog. Phys. 41 (1978) 1929–1967.

[6] P. Cheng, Heat transfer in geothermal systems, Adv. Heat Transfer 14 (1978) 1–105.

[7] M.A. Combarnous, S.A. Bories, Hydrothermal convection in saturated porous media, Adv. Hydrosci. 10 (1975) 231–307.

[8] G.Z. Gershuni, Y.M. Zhukhovitskiy, Vibration-induced thermal convection in weightlessness, Fluid Mech.-Sov. Res. 15 (1986) 63–84.

[9] P., Ghosh, Thermal-hydraulics of buoyancy-driven internal, external flows and flow through saturated porous medium under micro-gravity, PhD thesis, BHU, India, 2007.

[10] R.J. Gross, M.R. Bear, C.E. Hickox, The application of flux-corrected transport (FCT) to high Rayleigh number natural convection in porous medium, in: Proc. 8th International Heat Transfer Conference, San Francisco, CA, 1986.

[11] K. Hirata, T. Sasaki, H. Tanigawa, Vibrational effects on convection in a square cavity at zero gravity, J. Fluid Mech. 445 (2001) 327–344.

[12] Y. Kamotani, A. Prasad, S. Ostrach, Thermal convection in an enclosure due to vibrations aboard spacecraft, AIAA J. 19 (1981) 511–516.

[13] P.A. Kondos, R.S. Subramanian, Buoyant flow in a two-dimensional cavity due to a sinusoidal gravitational field, Microgravity Sci. Technol. 9 (1996) 143–151.

[14] D.M. Manole, J.L. Lage, Numerical benchmark results for natural convection in a porous medium cavity, in: Heat and Mass Transfer in Porous Media, ASME Conference, HTD, vol. 216, 1992, pp. 55–60.

[15] S. Mahmud, R.A. Fraser, Vibrational effect on entropy generation in a square porous cavity, Entropy 5 (2003) 366–376.

[16] S.L. Moya, E. Ramos, M. Sen, Numerical study of natural convection in a tilted rectangular porous material, Int. J. Heat Mass Transfer 30 (4) (1987) 741–756.

[17] X. Ruiz, L.R. Piscina, J. Casademunt, Numerical studies of fluid flow in microgravity conditions for confined crystal growth, Astrophys. Space Sci. 276 (2001) 135–140.

[18] K.L. Walker, G.M. Homsy, Convection in porous cavity, J. Fluid Mech. 87 (1978) 449–474.